# Oscillator-based walking assistance: Optimization & validation
## *Part II: Ankle joint validation*

C.S. Lintzen[a], W. van Dijk[a], R. Ronsse[b], J. van den Kieboom[c], A.J. Ijspeert[c], H. van der Kooij[a]

[a] *TU Delft, The Netherlands*
[b] *Université catholique de Louvain, Belgium*
[c] *EPFL Lausanne, Switzerland*

**Abstract**

A human with muscle weakness can wear a rehabilitation device, e.g. exoskeleton, to receive support during walking. However, how can this support be adjusted in real-time to the intention of the user? The given support should be intuitive, user-specific, compliant and robust to sensor noise. We suggest the use of an adaptive oscillator which can detect the frequency and phase of the user's gait. The designed oscillator-based controller is capable to adjust the support in real time, based on reliable joint angle measurements. The adaptive oscillator determines the position and velocity reference trajectories, based on the measured joint angles. The controller uses these reference trajectories to attract the current angle respectively velocity.

This is part II of a two-part paper. In part I of this paper the controller is optimized using simulations. In part II the performance of the optimized oscillator-based controller is determined for the ankle joint using specially designed pneumatic ankle foot orthoses (PAFO). The PAFO actuate the plantar flexion movement with pneumatic muscles. The performance of the controller is analyzed measuring the activity of the Tibialis Anterior and Gastrocnemius Medialis with electromyography (EMG).

The oscillator-based controller found the same reference joint angles and velocities in real time compared to the optimization. The desired exoskeleton torques are comparable to the simulations, but the amplitude is lower. The support decreased the EMG activity of the Gastrocnemius Medialis. However, the lack of transparency of the PAFO increased the EMG of the Tibialis Anterior.

Overall the oscillator-based controller can give a user-specific support by detecting the gait frequency and learning the gait trajectory. The specially designed PAFO can measure the performance of controllers on humans objectively. The EMG of the Gastrocnemius Medialis can decrease more, when the transparency of the PAFO is increased.

## 1. Introduction

The human capability to walk and stand on two legs has a lot of influence on his/her physical and mental health. When this capability is disturbed, robots can come in to regain the mobility. These robots, e.g. exoskeletons, should adapt their behavior to the intention of the user [10], so that the user can interact with the exoskeleton rather than react to it [12].

In this research a control strategy with compliant behavior is developed to provide intuitive support to a human with muscle weakness during steady state walking with an anthropomorphic exoskeleton. The designed oscillator-based controller is capable to adjust the support in real time, based on reliable joint angle measurements.

Ronsse et al. [9, 10, 11] developed an oscillator-based controller, which can support the gait without time delay, gives a user specific support and is robust to sensor noise. Preliminary experiments assisting rhythmic elbow movements showed a clear decrease in the electromyography (EMG) of the biceps and triceps.

Recently Ronsse et al. [9] used the same approach to assist the hip joint. The hip joint angle is measured and adaptive oscillators [1, 7] are used to learn and predict the joint angles in real time based on previous gait cycles. The predicted trajectories are used to attract the current joint angle by means of a proportional control and a manual tuned stiffness. In this manner the oscillator-based

control strategy is capable to adjust the support to the walking pattern of the user, by using only one sensor per joint (measuring the current joint angle).

In the first part of this paper [4] an oscillator-based controller was designed by optimizations to assist the hip, knee and ankle joint. The manual tuned stiffness and the phase shift are optimized parameters. In a one-stage optimization the control parameters were determined minimizing the power consumption, the stiffness of the controller and the disturbance of the gait. The simulation results showed that the designed control strategy is capable to assist steady state walking. However, the optimized controller may work in simulation, but a comfortable assistance is not assured in practice. Besides that, in this part the joint angles and velocities have to be learned in real time.

Therefore, the simulation results [4] are validated by experiments in this second part of the paper. The performance of the controller is analyzed for the ankle joint using specially designed pneumatic ankle foot orthoses (PAFO). The PAFO can be attached to the Lower extremity Powered Exoskeleton (Lopes) [13], which can assist the hip and knee joint. However, the support of the hip and knee joint are beyond the scope of this paper, but the approach described in this paper is valid for all three joints.

We want to achieve that the optimized oscillator-based controller in simulations can be used real-time in experiments. The EMG activity needs to decrease as an objective measure of the performance of this controller.

In this report first the oscillator-based control strategy and the experiments are explained in the methods, then the results are shown, the paper is concluded with a discussion and recommendations on the performance of the oscillator-based controller and the PAFO.

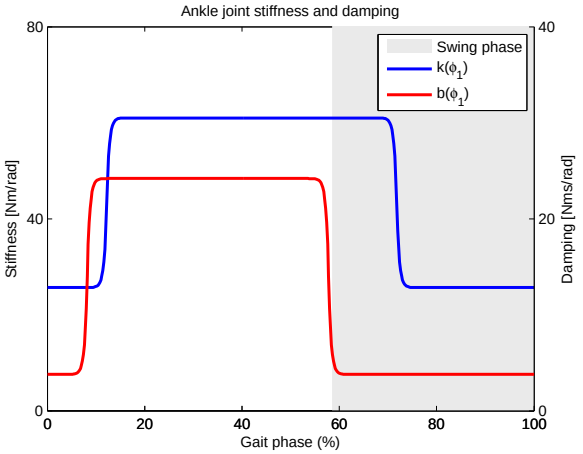


Figure 1: The stiffness and damping functions depend on the gait phase $\phi_1$. These functions were determined using optimizations in [4]

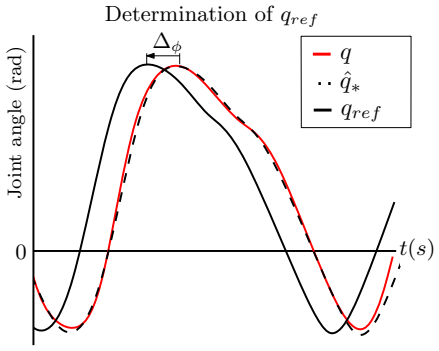


Figure 2: The joint angle $q$ is learned over multiple cycles to find the learned joint angle $\hat{q}_*$. This learned angle is shifted in phase with $\Delta_\phi$ to find the reference angle $q_{ref}$

## 2. Methods

In this paper the same oscillator-based controller is used as in [4] to validate the optimized controller on one subject. The oscillator-based controller uses a first order [3, 6] impedance control law to actuate the hip, knee and ankle joint in the sagittal plane with an exoskeleton torque $T_{exo}$:

$$T_{exo}(t) = \kappa\{k(\phi_1)\cdot(q_{ref}(t)-q(t)) + ... \\ b(\phi_1)\cdot(\dot{q}_{ref}(t)-\hat{\dot{q}}(t))\} \quad (1)$$

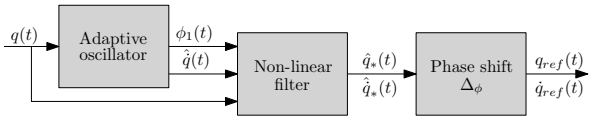


Figure 3: The adaptive oscillator can learn the phase $\phi_1$ and joint velocity $\hat{\dot{q}}$, based on the joint angle $q$. The non-linear filter finds the learned joint angle $\hat{q}_*$ and learned joint velocity $\hat{\dot{q}}_*$. These are shifted with an optimized phase shift $\Delta_\phi$ to find the reference angle $q_{ref}$ and reference velocity $\dot{q}_{ref}$

The measured joint angle $q(t)$ and calculated joint velocity $\hat{\dot{q}}(t)$ are compared to respectively a reference joint angle $q_{ref}(t)$ and reference joint velocity $\dot{q}_{ref}(t)$. The stiffness $k(\phi_1)$ and damping $b(\phi_1)$ functions are gait phase $\phi_1$ dependent and were determined by optimizations, see figure 1. The calculated torque $T_{exo}(t)$ is partly applied on the person, by means of multiplication with the support ratio $\kappa$.

The determination of the reference position $q_{ref}$ and reference velocity $\dot{q}_{ref}$ is unique for the oscillator-based controller. The starting point is that the joint trajectory should be adjusted in real time based on previous gait cycles. In figure 2 the determination of the reference angle $q_{ref}$ is shown. First the joint angle $q$ is learned from previous gait cycles, then the learned angle $\hat{q}_*$ is shifted in phase with an optimized factor $\Delta_\phi$ to find the reference angle $q_{ref}$.

In the simulations the gait phase $\phi_1$, the learned joint angle $\hat{q}_*$ and the learned joint velocity $\hat{\dot{q}}_*$ are known in advance, because steady state walking is assumed. However, in the experiments these variables are unknown and need to be learned.

In the experiments the oscillator-based controller has to detect the gait phase $\phi_1$, the learned joint angle $\hat{q}_*$ and the learned joint velocity $\hat{\dot{q}}_*$, an overview is shown in figure 3. Adaptive oscillators [1, 7] are used to detect the gait phase $\phi_1$ and estimate the joint velocity $\hat{\dot{q}}$, section 2.1. A non-linear filter [2] determines the learned joint angle $\hat{q}_*$ and the learned joint velocity $\hat{\dot{q}}_*$, section 2.2. The learned angle and velocity are used to find the reference angle by applying an optimized phase shift $\Delta_\phi$. The method is concluded with a section on the experimental protocol, section 2.3.

### *2.1. Adaptive phase oscillator*

An adaptive phase oscillator can learn a periodic input $F$. When the periodic input is learned, the oscillator can deliver a filtered phase $\phi_1$ in real time, used to apply the corresponding phase shift, stiffness and damping. In this section first a simple adaptive oscillator is explained, learning a sinusoidal input. Then a more sophisticated oscillator is explained learning non-sinusoidal inputs, used in this paper.

*Sinusoidal input.* The basic building block of the used adaptive phase oscillator is a modified Hopf oscillator, that can synchronize to a sinusoidal input $F$. The oscillator is similar to the one used by Righetti et al. [1, 7], but transferred to polar coordinates:

$$\dot{\phi} = \omega + \nu F cos(\phi) \tag{2}$$

Where $\phi$ is the phase of the oscillator, $\nu$ a constant determining the speed of synchronization to $F$ and $\omega$ the intrinsic frequency. The modified Hopf oscillator only synchronizes to the periodic input signal, to actually learn the frequency of the teaching signal $F$, the intrinsic oscillator frequency $\omega$ has to adapt:

$$\dot{\omega} = \nu F cos(\phi) \tag{3}$$

This equation implies that the sum of $\dot{\omega}$ over one period is zero, if the intrinsic frequency $\omega$ is equal to the frequency of the input signal $F$, i.e. the oscillator is converged. If the input signal is sinusoidal and the oscillator is synchronized to the input, the filtered learned signal $\hat{q}$ can be obtained by:

$$\hat{q} = \alpha_1 sin(\phi) + \alpha_0 \tag{4}$$

With the amplitude $\alpha_1$ and the offset $\alpha_0$ converging to the sinusoidal input characteristics of $q$. Righetti et al. [8] showed that this convergence is guaranteed, when the input of the adaptive oscillator $F$ becomes the difference between the actual signal $q$ and the already learned signal $\hat{q}$, i.e.: $F(t) = q(t) - \hat{q}(t)$. The offset and amplitude can then be learned by the integrators:

$$\begin{aligned} \dot{\alpha}_0 &= \eta F \\ \dot{\alpha}_1 &= \eta F sin(\phi) \end{aligned} \tag{5}$$

Where $\eta$ is the integrator gain. This modified Hopf oscillator can learn sinusoidal inputs $F$. The oscillator becomes a low-pass filter without delay, when the input signal $q$ consist of more frequencies.

*Non-sinusoidal, but periodic input.* The proposed adaptive oscillator can only learn one frequency. It is possible to learn periodic signals, which consists of multiple frequencies by using several adaptive oscillators in parallel [8]. Ronsse et al. [9] suggested that for a periodic input only the main frequency has to be learned, the others are multiples of it. In this case the equations 2-5 are changed to:

$$\begin{aligned} \dot{\phi}_i &= i\omega + \nu F cos(\phi_i) \\ \dot{\omega} &= \nu F cos(\phi_1) \\ \dot{\alpha}_i &= \eta F sin(\phi_i) \\ \hat{q} &= \sum_{i=0}^{K} \alpha_i sin(\phi_i) \end{aligned} \tag{6}$$

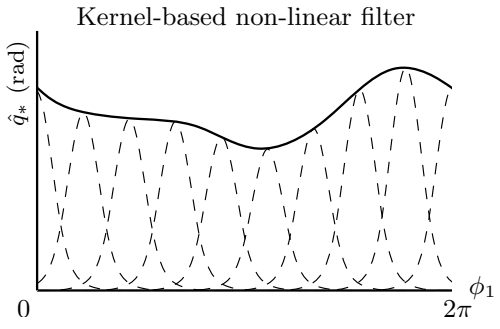


Figure 4: The learned joint angle $\hat{q}_*$ is determined by a kernel-based non-linear filter. The main phase $\phi_1$ divides the periodic input in $N$ equal parts. In each part $i$ a Gaussian function $\Psi_i$ is placed with corresponding weight factor $\gamma_i$ to find the learned joint angle $\hat{q}_*$

Where $\phi_i$ is the phase and $\alpha_i$ is the amplitude of oscillator $i$. The 0th integrator in equation 6 is still learning the offset, choosing $\phi_0(t) = \phi_0(0) = \pi/2$. The velocity $\hat{\dot{q}}$ can be estimated by taking the derivative of the sum of sinusoids:

$$\hat{\dot{q}} = \sum_{i=0}^{K} \dot{\alpha_i} sin(\phi_i) + \alpha_i \dot{\phi_i} cos(\phi_i) \tag{7}$$

The adaptive oscillator adapts fast to the input signal, when the constants are defined as follows: $\nu = 17$, $\eta = 0.25$ and $K = 10$.

### *2.2. Kernel-based non-linear filter*

The proposed adaptive oscillator in section 2.1 can learn sinusoidal signals. However, Ronsse et al. [9] found that a large number of oscillators are required to learn intervals in the joint signals, e.g. the plateau in the knee profile during the stance phase of walking. Therefore, the adaptive phase oscillator is combined with a kernel-based non-linear filter [2] to reduce the number of oscillators needed.

*Learning joint angle & velocity.* The kernel-based non-linear filter uses the main oscillator phase $\phi_1$ to divide the periodic input $q$ in $N$ equal parts between $0-2\pi$. In every part a Gaussian-like kernel function $\Psi_i$ is placed, defined by the width $h$ and the center $c_i$, see figure 4. The learned angle $\hat{q}_*$ is then the weighted sum of $N$ Gaussian-like kernel functions $\Psi_i$:

$$\begin{aligned} \hat{q}_*(\phi_1) &= \frac{\sum \Psi_i(\phi_1)\gamma_i}{\sum \Psi_i(\phi_1)} \\ \Psi_i(\phi_1) &= e^{hcos(\phi_1 - c_i) - 1} \end{aligned} \tag{8}$$

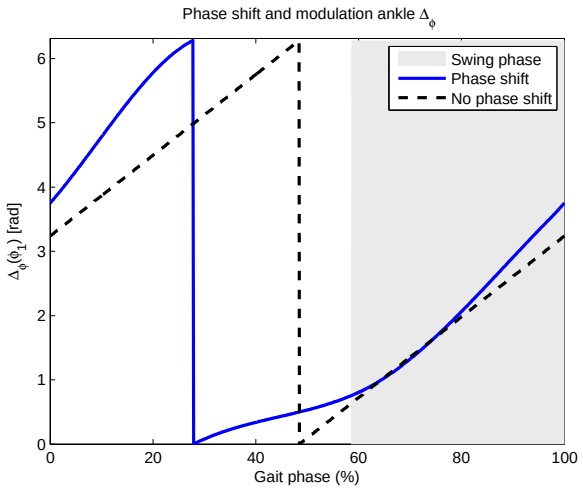


Figure 5: The phase shift $\Delta_\phi$ is phase dependent $\phi_1$ and was determined by optimizations [4]

The joint angle $q$ is mapped when the weight $\gamma_i$ minimize the quadratic error criterion for every Gaussian-like kernel function $\Psi_i$:

$$J_i = \sum_{k=1}^{M} \Psi_i(k)(q(k) - \gamma_i(k))^2 \tag{9}$$

Where $k \in [1, M]$ are the $M$ discrete time steps and $q(k)$ the signal to be learned. The quadratic error criterion $J_i$ can be minimized in real time using incremental regression [2], which is done with the use of recursive least squares with a forgetting factor of $\lambda$. The weight factors $\gamma_i$ can be updated by:

$$\begin{aligned} \gamma_i(k+1) &= \gamma_i(k) + \Psi_i(k) P_i(k+1)(q(k) - \gamma_i(k)) \\ P_i(k+1) &= \frac{1}{\lambda}(P_i(k) - \frac{P_i(k)^2}{\frac{\lambda}{\Psi_i(k)} + P_i(k)}) \end{aligned} \tag{10}$$

Where $P$ is the inverse covariance matrix [5]. Recent data is more important, if $\lambda < 1$ [9].

*Reference angle & velocity.* The reference angle $q_{ref}$ is found by applying a phase shift $\Delta_\phi$ to the learned joint angle $\hat{q}_*$:

$$\begin{aligned} q_{ref}(\Delta_\phi) &= \frac{\sum \Psi_{i,\Delta} \gamma_i}{\sum \Psi_{i,\Delta}} \\ \Psi_{i,\Delta} &= e^{hcos(\Delta_\phi - c_i) - 1} \end{aligned} \tag{11}$$

The reference velocity $\dot{q}_{ref}$ is determined in the same manner as the reference angle $q_{ref}$. The phase

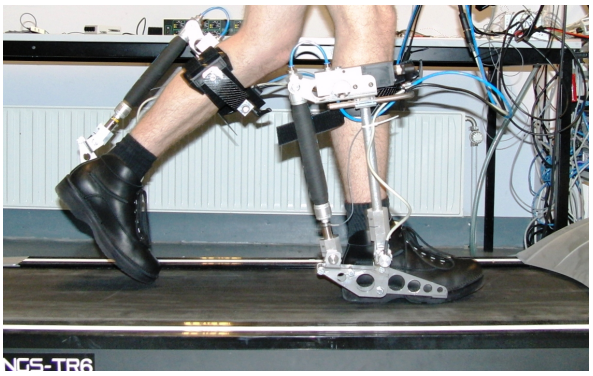

Figure 6: PAFO, pneumatic ankle-foot orthoses. The plantar flexion movement is actuated with a pneumatic muscle. An encoder and load cell measure respectively joint angle and force

shift $\Delta_\phi(\phi_1)$ is determined by optimizations and is defined as follows:

$$\Delta_\phi(\phi_1) = a_\phi + f(\phi_1) \tag{12}$$

The constant phase shift $a_\phi$ puts the reference angle in front of the measured angle. The addition of the phase modulation $f(\phi_1)$ makes small adjustments of the reference angle possible. In figure 5 the optimized phase shift is found. The same phase shift is used for both position as velocity, but the shift differs per joint.

The constants of the non-linear filter are defined to get a good fit as follows: $\lambda = 0.9995$, $N = 90$ and $h = 144$.

### *2.3. Experimental setup*

The optimized controller is tested on humans, actuating the plantar flexion movement of the ankle joint with a specially designed pneumatic ankle foot orthosis (PAFO).

*Experimental equipment.* The plantar flexion movement of the PAFO (figure 6) is actuated with a pneumatic muscle (Festo MAS-20-250N). The PAFO consists of two orthosis to support both the left as the right ankle, each orthosis weighs 3.5 kg.

Both orthoses are equipped with a load cell (Futek LCM200) and a proportional 5/3 way valve (Festo MPYE-5) to regulate the force generated by the pneumatic muscle and an absolute encoder (Baumer ATD 07 S A4) to measure the ankle joint angle. These sensors and the valve are connected to a Beckhoff EtherCAT system and Matlab xPC. Data is collected for post-hoc analysis with the same sensors at a frequency of 50 Hz.

The EMG of the Gastrocnemius Medialis and the Tibialis Anterior are measured with a Delsys Bagnoli EMG system to check the performance of the controller at a frequency of 500 Hz. The EMG data is synchronized with the EtherCAT system.

*Participant.* In this pilot test the performance of the oscillator-based controller is tested on one male participant (aged 25, weight 70 kg and length 1.90 m).

*Experimental protocol.* In total the performance of the optimized controller and PAFO is tested for five successive conditions. In every condition the participant walked 15 minutes on the treadmill (Hastings TR-6) with a speed of 3 km/h. The last 5 minutes of each condition were used for data analysis, so that the participant had 10 minutes to adapt to the support. The following conditions are used:

1. In the *free walking* condition the participant walks without wearing the PAFO, but with comparable heavy shoes. This condition is used to evaluate the EMG level of normal walking.
2. In the *zero impedance* condition the orthosis applies zero torque to determine the actual transparency of the PAFO. Actually the orthosis executes 1 Nm plantar flexion torque to increase the controllablity of the pneumatic muscle.
3. In the *20% support* condition, the PAFO delivers 20% of the total torque, 80% is generated by the person according the simulations ($\kappa = 0.2$).
4. In the *50% support* condition the PAFO delivers 50% of the total torque, 50% is generated by the person according the simulations ($\kappa = 0.5$).
5. In the *100% support* condition the PAFO delivers 100% of the total torque, 0% is generated by the person according the simulations ($\kappa = 1$).

## 3. Results

The results of the experiment are averaged over all steps to find a mean gait cycle and shown in figure 7-9.

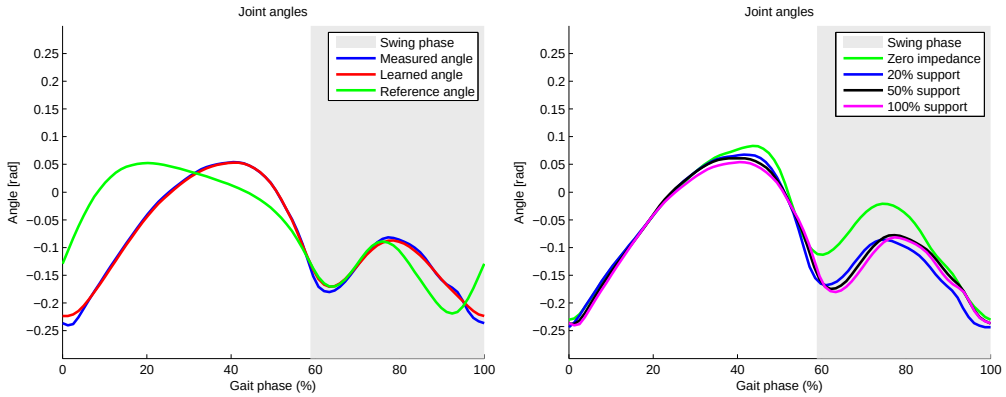


Figure 7: Mean ankle joint angle $q$. Left: Performance of the adaptive oscillator and non-linear filter in the 100% support condition; the joint angle $q$ is learned $\hat{q}_*$ and shifted to find the reference angle $q_{ref}$. Right: Performance of the oscillator-based controller, the measured joint angle $q$ is influenced by applying different support ratios and the PAFO

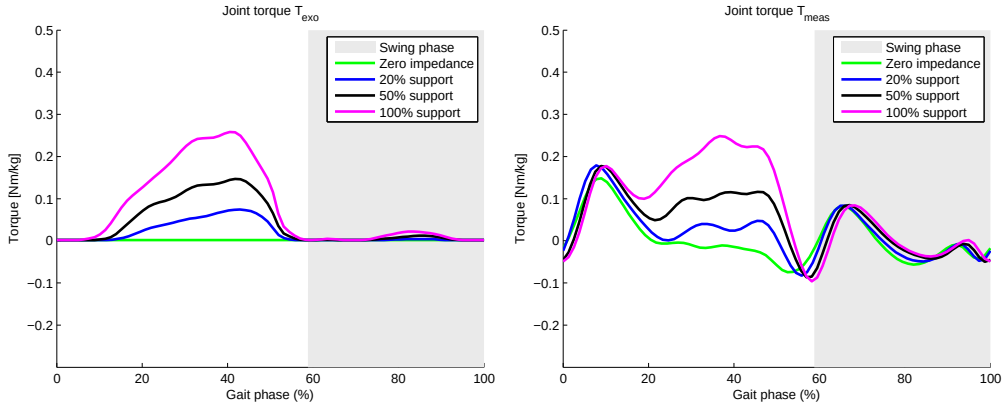


Figure 8: Mean ankle joint torques. Left: The exoskeleton torque $T_{exo}$ calculated by the oscillator-based controller. Right: Torque applied by the PAFO

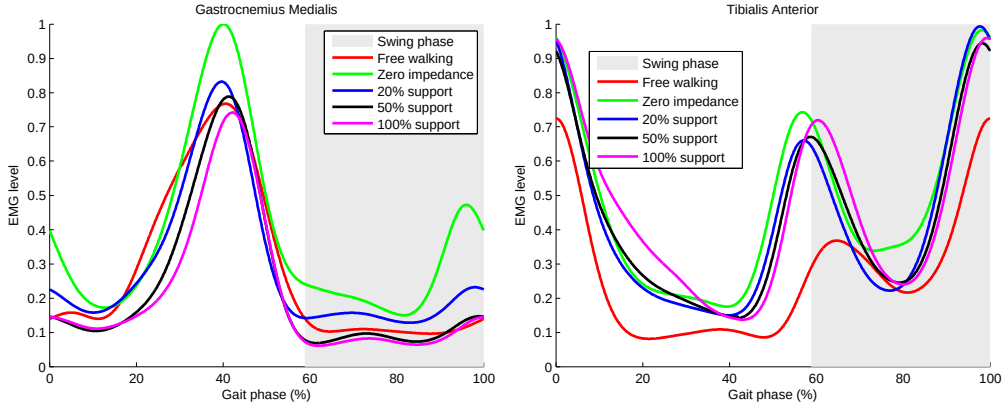


Figure 9: EMG level of the shank muscles with increasing support ratios. Left: Gastrocnemius Medialis. Right: Tibialis Anterior

The oscillator locks the frequency $\omega$ fast, in approximately 5 gait cycles. After the frequency is locked, the joint angle is learned accurately as can be seen in the left part of figure 7. The reference angle $q_{ref}$ is determined with the same phase shift $\Delta_\phi$ as in the simulations, but can now vary in real time based on the user's walking pattern. The stiffness and damping values are dependent on the gait phase and are automatically adjusted.

In the right part of figure 7 the influence of the *support* conditions is shown in comparison to the *zero impedance* condition. The joint angles during swing phase are clearly influenced by the orthosis. There is only a small difference between the different *support* conditions.

The left part of figure 8 shows the desired exoskeleton torque $T_{exo}$ in the plantar flexion direction calculated by the oscillator-based controller, equation 1. These torques have the same shape as the joint torques in the simulations [4], but the absolute value is 3.5 times smaller. Therefore, the actual support factors are approximately 5%, 12.5% and 25% instead of 20%, 50% and 100%.

The right part of figure 8 shows the executed torque by the PAFO. The torques applied in the *zero impedance* condition are not equal to 1 Nm, especially during early swing and stance. The increase of the desired exoskeleton torque over the different *support* conditions can be found back however.

In figure 9 the measured EMG levels are shown of the Gastrocnemius Medialis (plantar flexion) and Tibialis Anterior (dorsiflexion). According to an ANOVA test the differences, between the maximum EMG level of the Gastrocnemius Medialis for the different conditions, are significant with p¡0.05. There is a clear increase in EMG level between the *free walking* and *zero impedance* condition. This suggests again that the *zero impedance* condition is not transparent. This lack of transparency is clearly seen at early swing in the EMG level of the Tibialis Anterior. The EMG level of the Gastrocnemius Medialis decreases with increasing support ratio. The amount of decrease is however not linear.

## 4. Discussion

The discussion is divided into two parts, first the performance of the oscillator-based controller is discussed, second the performance of the PAFO is treated.

*Oscillator-based controller.* The conversion from simulations to experiments can be done quickly with the implementation of the oscillator-based controller in the Matlab environment. The optimized parameters can be loaded into the controller and the experiment can start instantaneously. The joint angles and velocities are learned in approximately 5 gait cycles and the reference angle and velocity are determined correctly and are comparable to the simulations.

The oscillator-based controller can adjust its support to the walking pattern of the user. The reference angle and velocity are adjusted such that the user can walk with varying speeds and with his/her specific trajectory.

The calculated exoskeleton torque $T_{exo}$ has the same pattern as the torque determined in the simulations, figure 8. The EMG level decreases with increasing support ratios $\kappa$, figure 9. The EMG decrease is however smaller than expected, this can probably be explained by a 3.5 times smaller exoskeleton torque $T_{exo}$ in the experiments than in the simulations. This is caused by an incorrect velocity determination in the simulations. The actual support rates are then 5%, 12.5% and 25% instead of 20%, 50% and 100%, which is the reason that the EMG decrease is small. Therefore, the EMG level of the Gastrocnemius Medialis in the *100% support* condition cannot be equal to zero, figure 9.

The oscillator-based controller neglectible influences the gait, the measured joint angles $q$ are approximately the same, see figure 7. However, in early swing the *zero impedance* condition has a clear difference in the measured joint angle compared to all *support* conditions. This is caused by the slow deflation of the pneumatic muscle, which is less inflated in the *zero impedance* condition.

Another notable aspect is the EMG increase in the *100% support* condition of the Tibialis Anterior around 10%-30% of the gait, figure 9. In early stance the knee is in full extension, if the pneumatic muscle then contracts, the knee threatens to go in hyperextension. This happens in the *100% support* condition. The hyperextension is prevented by contracting the Tibialis Anterior, which is seen as increase in the EMG level, figure 9. This problem is probably caused by the design of the PAFO. The PAFO tries to overtake the function of the Gastrocnemius Medialis. However, the Gastrocnemius Mediallis is a biarticular muscle, so that the knee cannot be overstretched.

The error torque $T_{error}$, introduced in the simula-

tion [4] to make the model walk feedforward stable, is not present during the experiments. Therefore the applied $T_{exo}$ in the experiments is more comparable to the Winter torques [14] then during the simulations.

*PAFO performance.* The increase in EMG activity in both muscles, switching from *free walking* to *zero impedance*, indicates that the PAFO is not really transparent, see figure 9. The measured joint torques confirm this lack of transparency, in the *zero impedance* condition the measured torque is not equal to 1 Nm, see figure 8.

The overall EMG increase of the Tibialis Anterior can partly be explained by the implementation of the pretension in the pneumatic muscle (1 Nm in plantarflexion direction). This pretension is implemented to increase the controllability of the pneumatic muscle. The addition of a spring in dorsiflexion direction can compensate for this 1 Nm torque.

In early swing phase there is one clear increase in the EMG of the Tibialis Anterior, comparing the *free walking* and the *zero impedance* condition. This peak is due to the slow deflation of the pneumatic muscle. At toe off the pneumatic muscle is fully inflated and to ensure ground clearance the pneumatic muscle has to deflate quickly. This problem can also be seen in the measured joint angle, which does not come above 0 rad during swing phase. This problem can be solved by increasing the diameter of the valve openings, e.g. by adding an exhaust valve.

## 5. Conclusion

The oscillator-based controller can give a user-specific support by detection of the gait frequency and determination of a user-specific reference trajectory. The optimized controller can be tested on humans using the specially designed PAFO. The EMG of the Gastrocnemius Medialis decreases significantly with increasing support ratio. However, the results need to be improved by increasing the transparency of the PAFO.

## 6. Future research

The transparency of the PAFO should be increased to make more reliable measurements. The exhaust of the pneumatic muscle should be faster, so that dorsiflexion is made easier at early swing. Pretension of the pneumatic muscle should be compensated by adding a spring in dorsiflexion. A local buffer in the hollow pipe of the PAFO can increase the bandwidth of the system. Besides improving the system dynamics, a better identification can improve the system behavior.

The performance of the controller was determined by testing the EMG levels of two shank muscles. However, the total gait pattern can be changed using the controller and the PAFO, A better performance measure for the controller would be the oxygen consumption, which can measure the total gait efficiency. Another option is to use more EMG electrodes, e.g. at the hip and knee muscles, to detect the changed gait pattern.

There is a clear difference between the ankle joint angles used in the optimization and the measured joint angles wearing the PAFO. The used joint angles in the simulation also vary from the Winter ankle joint angles [14]. The optimization can find a better controller by using comparable joint angles.

## References


[1] J. Buchli, L. Righetti, and A.J. Ijspeert. Frequency analysis with coupled nonlinear oscillators. *Physica D: Nonlinear Phenomena*, 237(13):1705–1718, 2008.

[2] A. Gams, A.J. Ijspeert, S. Schaal, and J. Lenarčič. Online learning and modulation of periodic movements with nonlinear dynamical systems. *Autonomous robots*, 27(1):3–23, 2009.

[3] N. Hogan. Impedance control: an approach to manipulation: parts 1, 2, 3. *Journal of Dynamic Systems, Measurement and Control*, 107:1–24, 1985.

[4] C.S. Lintzen, J. van den Kieboom, R. Ronsse, W. van Dijk, H. van der Kooij, and A.J. Ijspeert. Oscillator-based walking assistance: Optimization & validation. part i: Optimization by simulations. Master's thesis, TU Delft, 2011.

[5] L. Ljung and T. Söderström. Theory and practice of recursive identification. Technical report, The MIT Press Signal Processing, Optimization and Control Series, 1983.

[6] R. Riener, L. Lunenburger, S. Jezernik, M. Anderschitz, G. Colombo, and V. Dietz. Patient-cooperative strategies for robot-aided treadmill training: first experimental results. *IEEE Transactions on Neural Systems and Rehabilitation Engineering*, 13(3):380–394, 2005.

[7] L. Righetti, J. Buchli, and A.J. Ijspeert. Dynamic hebbian learning in adaptive frequency oscillators. *Physica D: Nonlinear Phenomena*, 216(2):269–281, 2006.

[8] L. Righetti and A.J. Ijspeert. Programmable central pattern generators: an application to biped locomotion control. In *Robotics and Automation, 2006. ICRA 2006. Proceedings 2006 IEEE International Conference on*, pages 1585–1590. IEEE, 2006.

[9] R. Ronsse, B. Koopman, N. Vitiello, T. Lenzi, Stefano Marco Maria De Rossi, and J. van den Kieboom. Oscillator-based walking assistance: a model-free approach. In *Proceedings of the 2011 IEEE International Conference on Rehabilitation Robotics (ICORR)*, pages 668–674. IEEE, 2011.

[10] R. Ronsse, N. Vitiello, T. Lenzi, J. van den Kieboom, M. Carrozza, and A. Ijspeert. Human-robot synchrony: flexible assistance using adaptive oscillators. *IEEE transactions on bio-medical engineering*, 58:1001–1012, 2011.

[11] R. Ronsse, N. Vitiello, T. Lenzi, J. van den Kieboom, M.C. Carrozza, and A.J. Ijspeert. Adaptive oscillators with human-in-the-loop: Proof of concept for assistance and rehabilitation. In *IEEE RAS and EMBS International Conference on Biomedical Robotics and Biomechatronics (BioRob)*, pages 668–674. IEEE, 2010.

[12] F. Sup, A. Bohara, and M. Goldfarb. Design and control of a powered transfemoral prosthesis. *The International journal of robotics research*, 27(2):263, 2008.

[13] J.F. Veneman, R. Kruidhof, E.E.G. Hekman, R. Ekkelenkamp, E.H.F. Van Asseldonk, and H. van der Kooij. Design and evaluation of the lopes exoskeleton robot for interactive gait rehabilitation. *IEEE Transactions on Neural Systems and Rehabilitation Engineering*, 15(3):379–386, 2007.

[14] D.A. Winter. *Biomechanics and motor control of human movement*. Wiley, 2009.